IEEE Access
Multidisciplinary | Rapid Review | Open Access Journal

Received July 23, 2021, accepted August 22, 2021, date of publication September 3, 2021, date of current version September 27, 2021.

Digital Object Identifier 10.1109/ACCESS.2021.3109960

An Integrated Technology of Ionospheric Backscatter Detection and Oblique Detection

PENG LOU[1,2], **LIXIN GUO**[1], **(Senior Member, IEEE), JING FENG**[2], **AND NA WEI**[2]

[1]School of Physics and Optoelectronic Engineering, Xidian University, Xi'an, Shaanxi 710071, China

[2]China Research Institute of Radio Wave Propagation, Qingdao, Shandong 266107, China

Corresponding author: Peng Lou (crirp_dep4_loupeng@163.com)

This work was supported by the Stable-Support Scientific Project of China Research Institute of Radiowave Propagation under Grant A131904W02.

ABSTRACT Traditional single ground-based ionospheric detection methods often fail to obtain accurately ionospheric parameter information due to the measurement errors of detection systems and inverse algorithms. With the development of high frequency communication and radar sounding techniques, the ionospheric combined detection technology with multi-means is the most effective way to obtain the more accurate ionospheric characteristics. In this study, combined with ionospheric backscatter detection and oblique detection methods, an integrated ionospheric detection technology (quasi-backscatter detection technology) is proposed. The ionospheric parameters are obtained based on the minimum mean square error criterion and global searching method. The experimental results show that the inversion accuracy of ionospheric parameters is significantly improved by using quasi-backscatter detection system(42.3°N, GeoM). In addition, we simulate the propagation characteristics of the quasi-backscatter detection system by using ray tracing technique. And the variation characteristics between the propagation mode (and the propagation energy) and the angle of the transmitting-receiving beam are obtained.

INDEX TERMS Ionosphere, quasi-backscatter detection, ionospheric detection ionogram, side-scatter.

I. INTRODUCTION

Using high frequency band electromagnetic waves reflected in the ionosphere, the capabilities of high-frequency radar systems and communication systems are utilized. The ionosphere as a transmission medium has time-varying dispersion characteristics. It changes significantly with solar activity, seasons, time, latitude and longitude, etc. The ionospheric real-time detection and information management are an indispensable part of the radar systems and communication systems [1]–[3].

At present, the commonly used ionospheric ground-based sounding systems include vertical detection, oblique detection, and backscatter detection. The vertical detection system can only be used to detect the ionospheric characteristics above the station [4]–[7]. The oblique detection system can only be used to detect the ionospheric characteristics by the point-to-point fixed circuit [8], [9]. The point-to-surface ionospheric detection can be achieved by backscatter detection system, which has the detection characteristics of long detection distance and wide coverage. In some areas where vertical detection and oblique detection equipment cannot be deployed, the backscatter detection systems are irreplaceable.

The working principle of the backscatter detection method is that the high-frequency radio waves are obliquely projected to the ionosphere and are reflected by ionosphere to the ground. The undulating characteristics of the earth's surface and the unevenness of the electrical characteristics cause the radio waves to be scattered in all directions. The wave will be obliquely projected to the ionosphere again and be reflected to the receiver of the backscatter detection system. The ionospheric backscatter detection ionogram is formed through echo signal processing [10], [11]. Due to the mixing of the reflected echoes from different ionospheric regions, it is technically difficult to only rely on the backscatter detection data for ionospheric propagation mode recognition and characteristic parameter inversion [12]–[14]. The propagation mode recognition can be utilized by the fusion of the multiple ionospheric detection data. Due to the time inconsistency of various ionospheric detection data, certain approximate processing methods are used for data fusion,

The associate editor coordinating the review of this manuscript and approving it for publication was Venkata Ratnam Devanaboyina.

resulting in errors in the ionospheric propagation mode recognition results [15]–[20].

An integrated ionospheric detection technology, combined with ionospheric backscatter detection and oblique detection methods, is proposed in this paper. This is a new concept of ionospheric detection technology, called quasi-backscatter detection technology, for obtaining long-distance and large-area ionospheric information. Through once electromagnetic wave emission, ionospheric backscatter detection echoes and oblique detection echoes are simultaneously received by the receivers in the backscatter detection area, which improves the utilization rate of system and provides a sufficient dataset for the inversion of ionospheric parameters.

The quasi-backscatter detection technology provides a new detection method for ionosphere environmental diagnosis. Using the quasi-backscatter detection system, the ionospheric integrated detection can be achieved based on less equipment. The conditions (such as radio wave coverage area, maximum useable frequency, etc.) on specific circuits of high-frequency radio waves can be monitored, determined, and predicted. The propagation hops distance and the variation features with time under the influence of different geophysical factors can be determined. It provides an important frequency selection basis for the communication and radar frequency management system. In addition, through the detection data inversion, the characteristic parameters of the ionosphere are obtained, and the three-dimensional electron concentration distribution can be reconstructed in the detection area. At the same time, this ionospheric information is the basis of real-time frequency selection for target detection, and can also be used to improve the accuracy of target positioning in radar systems by using ray tracing technology [21]–[26].

II. MATERIALS AND METHODS

The research on the propagation characteristics of ionospheric backscatter has been carried out by relevant researchers, and certain research results have been obtained [13], [14]. The research on the propagation characteristics of ionospheric quasi-backscatter is almost blank. With the development of high-frequency technology applications, this is a significance to research the propagation characteristics of ionospheric side scattering. Thus, we built the quasi-backscatter detection experimental platform. Based on the platform, the quasi-backscatter detection experiment is systematically carried out, and the ionogram for quasi-backscatter detection is obtained for the first time.

The equipment layout, system composition, and working methods of the ionospheric quasi-backscatter detection experimental platform are described in detail in this paper. The sketch map showing the radio waves propagation process of backscatter and quasi-backscatter is presented in Figure 1.

A. EXPERIMENTAL PLATFORM DISPOSING

Generally, the transmitting and the receiving station of the backscatter detection system are located at the same location, or there are separated to avoid the interference of the transmitting device to the receiving device [27]. The distance between the transmitting station and the receiving station is generally about 50km to 100km. In order to obtain the quasi-backscatter detection signal mentioned in this article, the transmitting station uses an array antenna and the receiving device is located in the backscatter coverage area. A wide-beam receiving antenna is used to simultaneously detect the regional ionosphere. Equipment resources are fully utilized to reduce system complexity.

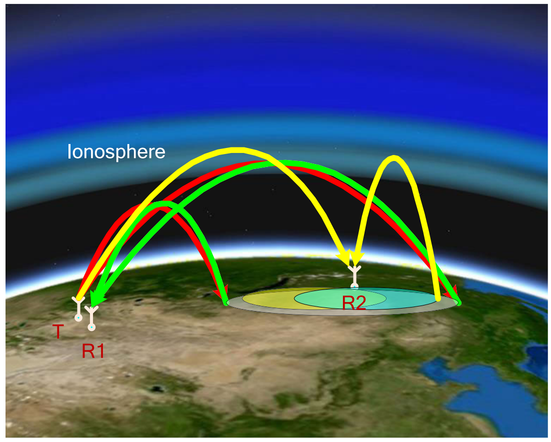

FIGURE 1. A map showing the radio waves propagation process of backscatter and quasi-backscatter.

Figure 2 shows the disposing situation of the quasi-backscatter detection experimental platform. The receiving antenna of the front receiving station R2 is an omni-directional antenna array. The eight channel (No.1 to No.8) were selected to deploy broadband receivers for detection.

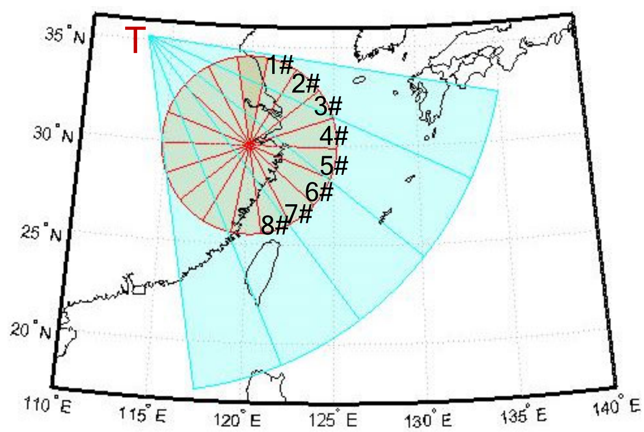

FIGURE 2. Schematic diagram of quasi-backscatter detection experimental platform.

B. EXPERIMENTAL PLATFORM COMPOSITION

The transmitting equipment mainly includes transmitting antenna, transmitter, detection signal generator, timing system, etc. The receiving equipment mainly includes receiving antenna, analog and digital receiver, timing system, data

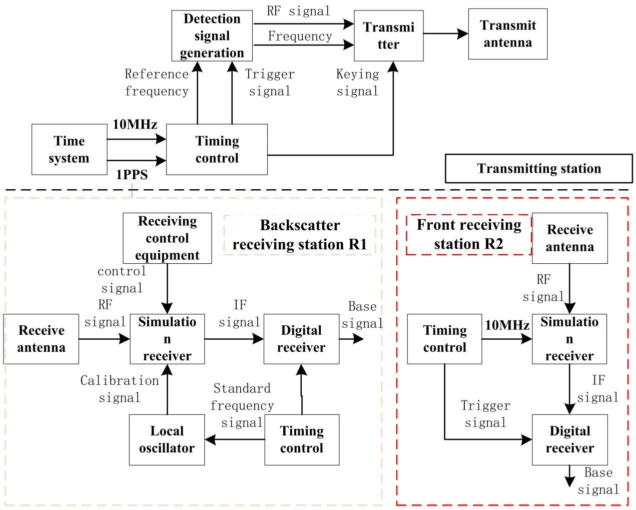

FIGURE 3. Schematic diagram of the experimental platform composition.

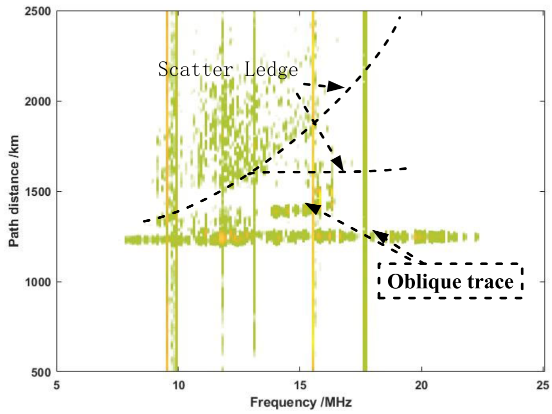

FIGURE 4. Experimental data of ionograms by pre-reception on 10 August 2020.

recording system, etc. The basic diagram of the system composition is shown in Figure 3. The synchronization method between the transmitting station and the receiving station is Global Position System (GPS) synchronization.

The working mode of the system is pulse compression. In order to obtain detection results with high range resolution, a detection pulse signal with a relatively wide bandwidth and low peak power is emitted. Linear Frequency Modulation Pulse (LFM) is the earliest proposed signal waveform based on pulse compression technology. It has been successfully applied to the conventional ionospheric backscatter detection system [28]. Since the range resolution is inversely proportional to the signal bandwidth, a signal with a larger bandwidth needs to be transmitted to improve the range resolution. Due to the influence of the ionosphere, and the HF band interference is more serious [29]–[31], the signal bandwidth is limited. After the verification of the experiment, the detection signal bandwidth is selected by 20kHz, and the pulse width is 4ms. The pulse repetition period is 50ms.

Through the working sequence design, several transmit wave positions can cover 60 degrees sector based on the phased array beam synthesis technology [32].

III. EXPERIMENT DATA ANALYSIS

A. OBSERVED DATA

On August 10, 2020, the three-dimensional sweep frequency ionogram obtained by the platform is shown in Figure 4. The x-axis of the ionogram is the working frequency (frequency range is 5MHz∼25MHz), and the y-axis is the group-path distance which is the product of the group time delay from the transmitting station to the receiving station and the light speed. The color is the strength of the received signal echoes. It can be seen from the ionogram that the ionogram contains both the oblique signal from the transmitter station to the receiver station and the scattered signal from the ordinate is the group-path distance is from the transmitting station through the ionospheric reflection to the receiving stations. For scattered signals, the group-path distance refers to the sum of the path distance from the transmitting station to the scattering point and the path distance from the scattering point to the receiving station.

The detection system adopts the sweep frequency detection. Through the research of signal detection algorithm, signal processing basic signal processing framework, interference rejection and other methods, an oblique detection ionogram and backscatter ionogram can be simultaneously extracted from the quasi-backscatter detection system. That is, information such as the radio wave propagation mode, radio wave coverage area, and optimal working frequency band in the area can be acquired through a frequency sweep detection.

In the coverage area of backscatter, different frequencies and types of echo signals are acquired based on the wide-beam receiving device. The signal has both oblique detection, side-backscatter and backscatter echo signals. The three-dimensional ionogram of the signal received by the 1# antenna 8# antenna is shown in Figure 5. In the figure, the oblique detection, side-backscatter and backscatter echo signals are simultaneously obtained. In the summer, it can be clearly seen from the oblique trace and the backscatter trace in the figure that the ionosphere Es layer echo is exist, and its path distance is about 1240km.

The 1# and 2# antenna directions of the receiving station are relatively close to the transmitting station, so the oblique signal received by the 1# and 2# antennas is relatively strong. The energy of the oblique signal is much higher than that of the scatter signal. Even if the range sidelobes are suppressed by the windows [32]–[34], it is still very strong relative to the noise and scatter signals [35]–[37]. Therefore, the sidelobes of the oblique signal received have a great influence on the extraction of the scattered signal.

Although the absorption loss at the low-frequency side of the short-wave band is stronger, and the gain of the transmitting and receiving antenna of the platform is larger at

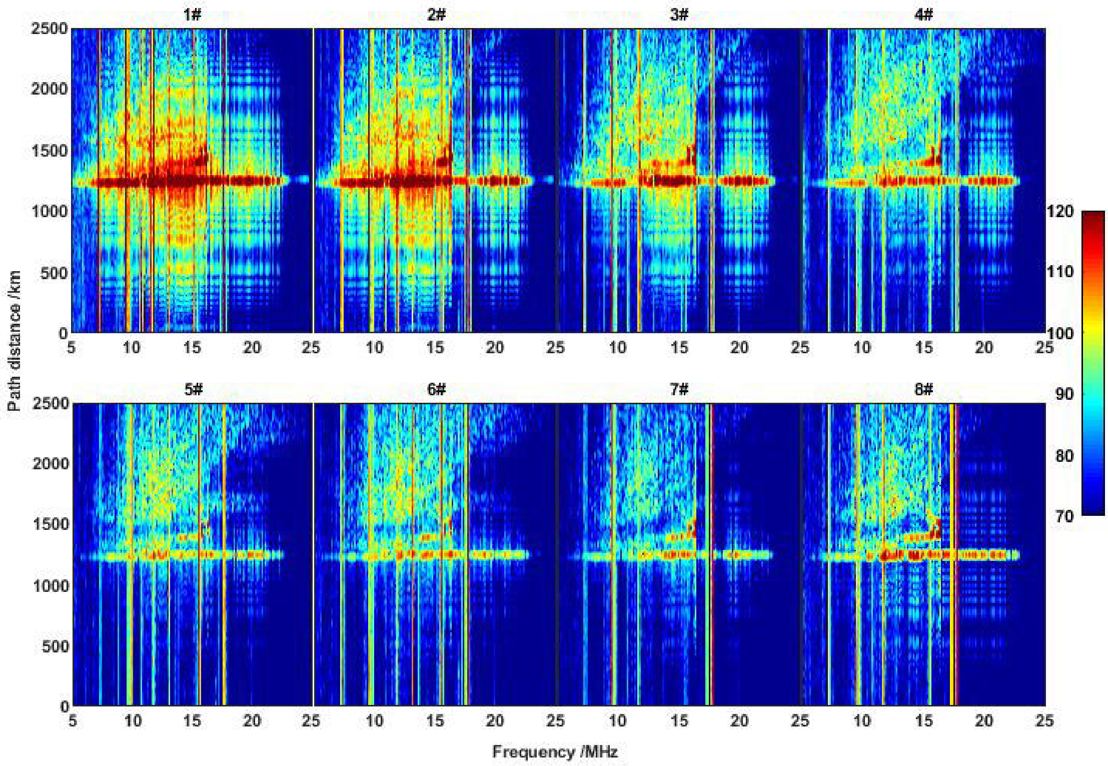

FIGURE 5. A series of three-dimensional ionograms observed by the front receiving station with different antenna orientations on 10 August 2020.

the high-frequency side, it can be seen from the figure that the energy of the scattered signal at the low-frequency side is stronger than that of the high-frequency side. The reason may be:

(1) The radio wave propagation path distance is relatively small at the low-frequency side, and the free space loss is relatively small [38]–[43];

(2) The signal energy at the low-frequency side is the superposition by the signal energy of two propagation modes (Es and F propagation modes).

B. JOINT INVERSION

By using the quasi-backscatter detection system, the ionospheric oblique detection and backscatter detection is simultaneously carried out. The ionosphere in the same area is detected by two different detection methods. Compared with conventional backscatter detection, the instability of the inversion algorithm for ionospheric characteristic parameters can be improved by the data fusion of the ionospheric oblique detection and backscatter detection.

In this paper, the "model" method is used for joint inversion of ionospheric parameters. It is to assume that the ionospheric electron density profile has a certain form and the model parameters are determined by inversion algorithm. In the process of joint inversion, the quasi-parabolic (QP) model is selected as the ionosphere background model in this paper [44], [45]. The three ionospheric parameters of the critical frequency f_c, bottom height r_b, and half thickness y_m in QP model are ultimately determined.

The ionosphere electron density profile of the QP model is given by:

$$N_e = \begin{cases} N_m\left[1-\left(\frac{r-r_m}{y_m}\right)^2\left(\frac{r_b}{r}\right)^2\right], & r_b < r < r_m\left\{\frac{r_b}{r_b-y_m}\right\} \\ 0, & \text{other} \end{cases} \tag{1}$$

where r_m, r_b, y_m are the peak height of the Electron density, bottom height, half thickness, respectively. The r_m satisfies $r_m = r_b+y_m$. N_m is the Electron density peak, $N_m = f_c^2/80.6$.

Considering the time-varying characteristics of the ionosphere, the linear gradient model is used to describe the ionospheric characteristic parameter distribution in the coverage area [46], [47]. Ionospheric parameters are functions of distance direction (θ) and azimuth direction (ϕ), described by:

$$f_p^2(r,\theta,\phi)=f_c^2(\theta,\phi)\left[1-\left(\frac{r-r_m(\theta,\phi)}{y_m(\theta,\phi)}\right)^2\left(\frac{r_b(\theta,\phi)}{r}\right)^2\right] \tag{2}$$

The ionospheric parameters change with distance direction θ is considered and the effect of ϕ is ignored. It ensures that the radio wave propagate in the great circle plane.

The gradient model is described by:

$$f_c(\theta) = f_{c0}(1 + G_f R_0 \theta) \tag{3}$$

$$h_m(\theta) = h_{m0}(1 + G_h R_0 \theta) \tag{4}$$

Here, G_f is the gradient of the critical frequency in the θ direction, G_h is the gradient of the height corresponding to the peak electron density in the θ direction, and R_0 is the radius of the earth.

The joint inversion method proposed in this paper adopts the ''minimum mean square error criterion''. On the ionogram, k frequency points are selected as f_i, and the corresponding k group-path observation values are $P'(f_i)$. The group-path calculated according to the ionospheric model parameters is $P\left(f_i, \bar{\xi}\right)$, and the mean square error between the calculated value and the observed value is shown in equation (5).

$$\varepsilon^2(\bar{\xi}) = \frac{1}{K}\sum_{i=1}^{K}\left(P'(f_i) - P(f_i, \bar{\xi})\right)^2 \tag{5}$$

where, $\bar{\xi}$ is the ionospheric parameter vector. The process of inversion is to find a $\bar{\xi}$, where $\varepsilon^2\left(\bar{\xi}_0\right)$ is the minimum value.

Based on the minimum mean square error criterion, K_1 and K_2 frequency points on the lead-edge of the backscatter and the oblique ionogram are selected respectively. The group-path observation value on the corresponding backscatter ionogram front is P'_{1i}, and the group path P_{1i} is calculated. The observed value of the group path on the corresponding oblique ionization diagram is P'_{2i}, and the group path P_{2i} is calculated. The mean square error ε between the calculated value and the observed value can be expressed as:

$$\varepsilon^2 = \frac{1}{K_1 + K_2}\left[\sum_{i=1}^{K_1}(P'_{1i} - P_{1i})^2 + \sum_{i=1}^{K_2}(P'_{2i} - P_{2i})^2\right] \tag{6}$$

Suppose the solution space is Φ, then $(f_c, r_b, r_m) \in \Phi$. First, the solution space Φ is determined by prediction or experience. Then, the global search is carried out in the solution space, and the mean square error is calculated. The optimal solution is obtained when the mean square error is the smallest.

Considering the time-varying characteristics of the ionosphere, the ionospheric parameter distribution often has a gradient trend. In order to simplify the inversion of gradient parameters, it is assumed that the ionosphere only has a linear horizontal gradient in the detection direction. According to the ionospheric gradient model, two parameters G_f and G_h need to be determined eventually. In the gradient inversion process, f_c, r_b, r_m have been obtained through the inversion of the vertical ionograms. By the minimum mean square error criterion, the corresponding optimal gradient value can be obtained through the global search method.

In this study, 10 consecutive cycles of ionospheric detection data are selected. The ionospheric characteristic parameters are the true values, which are obtained by the A Stations-Net of the National Radio Environment Monitor in the area near the oblique detection receiving station formed under the quasi-backscatter detection system.

Among, the inversion result of the vertical detection ionogram obtained by the vertical detection station which is near the oblique detection receiving station is taken as the ''real'' inversion result. And the electron density profiles obtained by different inversion methods are compared. The result is shown in Figure 6. The abscissa of The electron density vertically distribution obtained by inverting is the plasma frequency, and the ordinate is the ionosphere height.

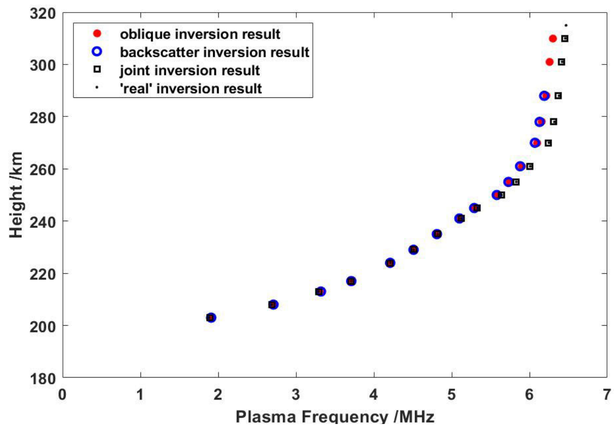

FIGURE 6. The deviation of electron density profile inverted compared between the "real" inversion result with different inversion methods.

Some examples of joint inversion results are shown in Table 1.

The sketch map showing the radio waves propagation process of backscatter and quasi-backscatter is presented in Figure 1. The ionospheric characteristic parameters are the true values, which are obtained by the A Stations-Net of the National Radio Environment Monitor (the V1 in the Figure 7) in the area near the oblique detection receiving station formed under the quasi-backscatter detection system.

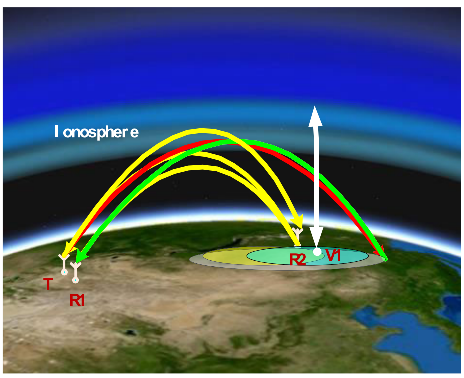

FIGURE 7. A map showing the radio waves propagation process of backscatter and quasi-backscatter.

The method for electron density profile inversion of oblique detection echoes in the integrated ionospheric detection ionogram is adopted in this paper [7], [53]. The group-path (p') and ground distance (D) integrals for spherical

TABLE 1. Statistic of QP model parameters obtained by different inversion methods.

	Oblique inversion result			Backscatter inversion result			Joint inversion result		
Serial number	f_c [MHz]	r_b [km]	r_m [km]	f_c [MHz]	r_b [km]	r_m [km]	f_c [MHz]	r_b [km]	r_m [km]
1	5.6	202.5	283.0	5.8	237.0	294.0	6.2	201.0	310.5
2	5.3	203.5	269.0	6.8	202.5	346.0	6.0	202.0	299.5
3	6.0	202.0	299.5	4.9	176.5	241.5	6.1	201.5	304.0
4	7.1	201.5	347.0	6.2	189.0	311.5	5.9	202.5	293.5
5	6.6	201.5	324.0	6.6	189.5	339.0	5.6	203.0	279.5
6	6.9	201.0	343.0	5.1	168.0	252.0	5.9	203.5	294.0
7	5.2	206.5	266.5	6.6	193.5	337.0	6.3	201.5	317.0
8	5.9	200.0	292.0	6.6	194.0	338.0	5.6	200.5	280.0
9	6.8	197.5	342.0	5.7	232.5	289.5	6.0	200.0	300.5
10	5.3	200.5	269.0	5.8	210.0	289.5	6.1	197.5	305.5
Standard deviation	0.73			0.66			0.23		

symmetry and no magnetic field are easily found as:

$$p'/2 = (R_t/\cos\beta_0)\left[\sin\chi_t + R_t\left(D/2 - \chi_t\right)\right] \tag{7}$$

where

$$\chi_t = -\beta_0 + \cos^{-1}(\cos\beta_0/R_t) \tag{8}$$

With the Newton-Raphson homing procedure, ionospheric electron density profiles in the area near the midpoint of the oblique detection link formed under the quasi-backscatter detection system were constructed by the ionosphere QP model. The oblique inversion result is shown in Table 1.

It is a common inversion method to make only use the leading edge of backscatter detection echoes in the integrated ionospheric detection ionogram. The ionospheric model of horizontal ionospheric inhomogeneity is used, which is characterized by the height of the electron density peak not depending on the distance from the observing point. The electron density distribution in the direction of sounding is specified as [30], [54]:

$$N(h, x) = N_0(h)\left[1 + u(x)\right] \tag{9}$$

Fridman developed a technique to determine the horizontal structure of the ionosphere by solving nonlinear problems with Newton-Kontorovich method and linear ill-posed problems with Tikhonov regularization method [30], [54]. The backscatter inversion result is shown in Table 1.

The ionospheric model of horizontal ionospheric parameters change is used as equation (3) and (4). The ionospheric parameters change with distance direction θ is considered and the effect of ϕ is ignored. It ensures that the radio wave propagate in the great circle plane. The initial parameters value of the ionospheric critical frequency f_{c0}, peak height h_{m0} in QP model are ultimately determined by the oblique inversion result. The inversion method of Fridman is improved by increasing inverted frequency range gradually in this paper [55]. The frequency range of the backscattered echo in the integrated ionospheric detection ionogram is divided into several frequency bands. The frequency band used in each inversion is added to the frequency band used in the previous inversion. Moreover, the initial electron density profile of each inversion is taken as the result of the previous inversion. It limits the solution space of the inversion. Determining the demarcation points of the inversion results in different frequency intervals and the continuity and smoothness of the inversion results can be avoided. The prior information can be used well to constrain the inversion solution. The real solution is gradually approximated to improve the accuracy of the inversion. Compared with the traditional inversion algorithm using the backscattered echo minimum group delay with the full-band frequency, the frequency is gradually approached and the inversion is not only able to see the "general view" of the ionosphere. The "overview" of the ionosphere can be obtained by the inversion method of increasing inverted frequency range gradually. The "details" of the ionosphere changing characteristics were discovered. Therefore, this method has higher inversion accuracy.

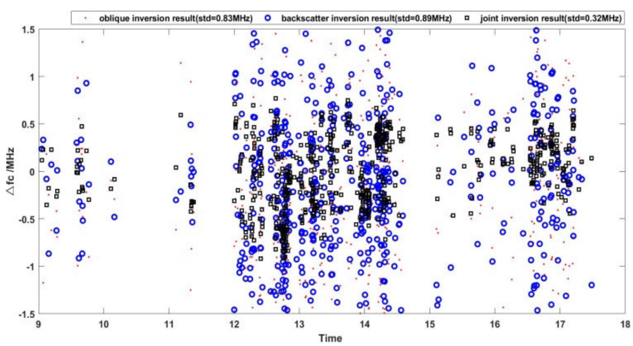

FIGURE 8. The deviation distribution of ionospheric F2 layer critical frequency inversed by different inversion methods.

In August and October 2020, the quasi-backscatter detection experimental platform was used to carry out continuously ionospheric joint detection experiments. The detection data is accumulated and processed, and the inversion accuracy of the ionospheric characteristic parameters is verified. For the accumulated 601 detection data, the inversion accuracy of different inversion methods is counted. It is shown in Figure 8 and Figure 9.

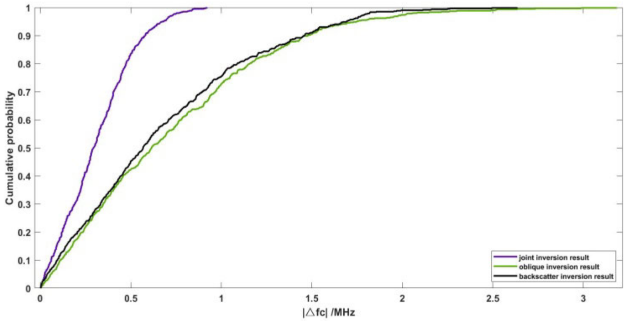

FIGURE 9. The deviation cumulative probability distribution of ionospheric F2 layer critical frequency inversed by different inversion methods.

Compared with other inversion methods, the inversion algorithm accuracy (critical frequency) has increased about 64% based on the quasi backscatter system. The probability of critical frequency deviation less than 0.5 MHz is greater than 85%, which is about 102% higher than other inversion methods. Preliminary experimental results show that the inversion algorithm accuracy can be significantly improved based on the quasi backscatter system and joint inversion of backscatter and oblique ionograms.

C. SCATTERING CHARACTERISTICS SIMULATION

The receiving device arranged in the backscatter coverage area is a wide beam receiving device. Due to the different positions of the transmitting station and the receiving station and the inhomogeneity of the ionosphere, the propagation paths of the radio waves from the transmitting station to the scatter unit and from the scatter unit to the receiving station must be different. Therefore, the calculation of the path parameters of the side-scatter and backscatter is relatively complicated.

Based on the ionospheric model, three-dimensional digital ray tracing technology is used in this paper [24], [48], [49]. With regard to the azimuth angle within the transmitted beam, the positions (latitude and longitude) of all scatter units are determined according to the ground distance of the obtained radio wave propagation path. For all scatter units, the corresponding receiving azimuths are calculated, and the scattering units in the receiving beam are reserved; For the reserved scatter unit, the ground distance to the receiving station is calculated separately. Whether the ground distance is included in the radio wave propagation path in the corresponding receiving azimuth is searched. If included, the side-scatter path is considered to exist; the parameters of the side scattering path are recorded, and the parameters mainly include the position of the scatter unit, the launching elevation angle, the path distance from the transmitting station to the scatter unit and the marking of the reflective layer, and the path distance from the transmitting station to the scatter unit, the reflection layer mark, and the receiving elevation angle.

In addition to the oblique detection echo, the ionospheric echo obtained by the front receiving station includes echoes such as side scatter and backscatter. Like the backscatter, the side-scatter echo energy is the superposition of a large number of possible ionospheric path incoming wave energy. The calculation of the wave energy for side scattering is more complicated.

It is supposed that a narrow beam is emitted by a transmitter located at T on the surface of the earth. The beam elevation angle is β_t, the beam elevation angle width is $\Delta\beta_t$, the azimuth angle is ϕ_t, and the azimuth angle width is $\Delta\phi_t$. Then the solid angle of beam can be expressed as:

$$\Delta\Omega_t = \cos\beta_t \Delta\beta_t \Delta\phi_t \tag{10}$$

The beam is reflected by the ionosphere to the Q position on the earth's surface. Then the area corresponding to solid angle $\Delta\Omega_t$ is:

$$\Delta S_t = r_0 \frac{\partial D_t}{\partial \beta_t} \sin\beta_t \sin\frac{D_t}{r_0} \Delta\beta_t \Delta\phi_t \tag{11}$$

where, D_t is the ground distance from the launch point T to the Q. Then the equivalent path distance of radio wave propagation is:

$$d_t = \left(\frac{\Delta S_t}{\Delta\Omega_t}\right)^{\frac{1}{2}} = \left(r_0 \frac{\partial D_t}{\partial \beta_t} \sin\beta_t \sin\frac{D_t}{r_0} \Big/ \cos\beta_t\right)^{\frac{1}{2}} \tag{12}$$

The corresponding ground area of ΔS_t is:

$$\Delta\gamma = \Delta S_t / \sin\beta_t \tag{13}$$

The equivalent propagating path distance of the radio wave scatter from Q to the receiving station at R on the earth's surface is:

$$d_r = \left(\frac{\Delta S_r}{\Delta\Omega_r}\right)^{\frac{1}{2}} = \left(r_0 \frac{\partial D_r}{\partial \beta_r} \sin\beta_r \sin\frac{D_r}{r_0} \Big/ \cos\beta_r\right)^{\frac{1}{2}} \tag{14}$$

where, $\Delta\Omega_r$ is the solid angle of the beam from Q to R, ΔS_r is the area, D_r is the round distance, β_r is the elevation angle of the scatter beam that can reach R.

Therefore, when the path distance is x, the signal energy of the specified frequency received at R is [50]–[52]:

$$\begin{aligned} P_r(x) &= \int_{coverage\ area} \frac{P_t G_t}{4\pi\left(\frac{\Delta S_t}{\Delta\Omega_t}\right)} \times \frac{\sigma\Delta\gamma}{4\pi\left(\frac{\Delta S_r}{\Delta\Omega_r}\right)} \times \frac{\lambda^2 G_r}{4\pi} \\ &= \int_{coverage\ area} \frac{\lambda^2 P_t G_t G_r}{(4\pi)^3} \times \frac{\sigma}{\sin\beta_t} \\ &\quad \times \frac{\cos\beta_r}{r_0 \frac{\partial D_r}{\partial\beta_r} \sin\beta_r \sin\frac{D_r}{r_0}} \cos\beta_t \mathrm{d}\beta_t \mathrm{d}\phi_t \end{aligned} \tag{15}$$

where P_t is the average transmit power, G_t and G_r are the transmit antenna and receive antenna gains, respectively. The antenna gains are functions of f (operating frequency), β_t and ϕ_t. λ is the wavelength, and σ is the scattering coefficient per unit ground area.

The antenna gain is simulated using Gaussian pattern function. The Gaussian pattern function is:

$$F(\beta,\phi) = \exp\left(-\left(\frac{\beta-\beta_0}{\beta_{3\mathrm{dB}}}\right)^2 - \left(\frac{\phi-\phi_0}{\phi_{3\mathrm{dB}}}\right)^2\right) + F_0 \tag{16}$$

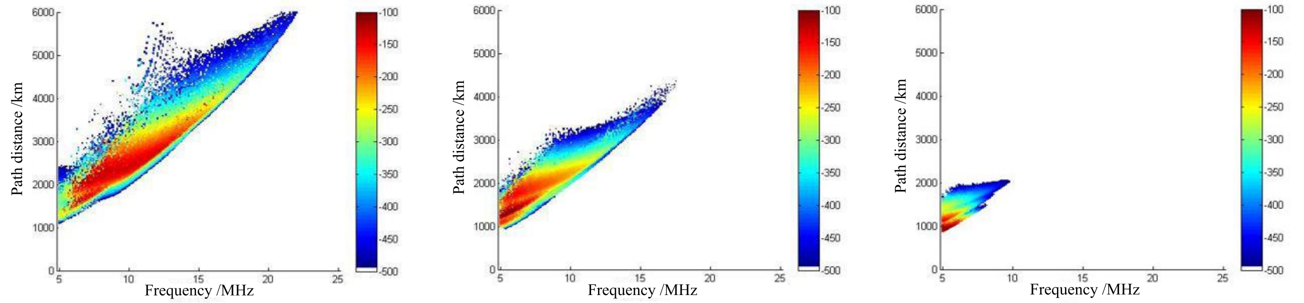

(a) receiving main beam directions is 90° **(b) receiving main beam directions is 120°** **(c) receiving main beam directions is 150°**

FIGURE 10. Simulation of scatter characteristics with a series of receiving main beam directions by the fixed transmitting beam directions.

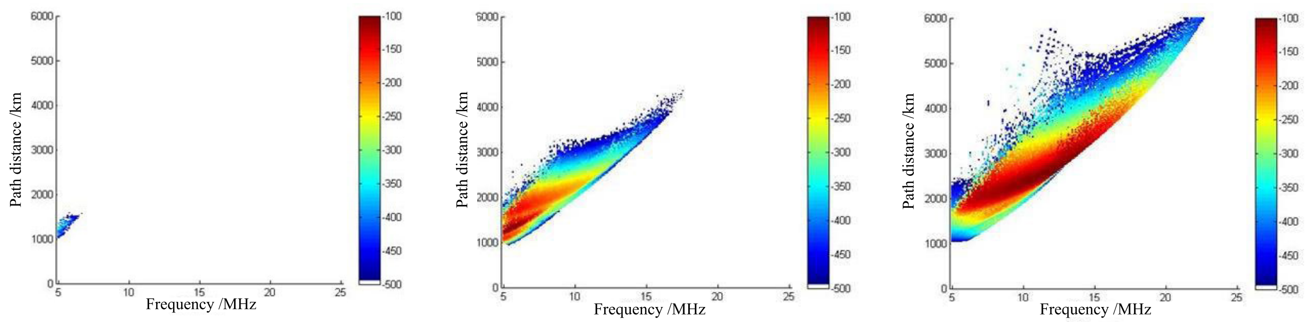

(a) transmitting main beam directions is 90° **(b) transmitting main beam directions is 120°** **(c) transmitting main beam directions is 150°**

FIGURE 11. Simulation of scatter characteristics with a series of transmitting main beam directions by the fixed receiving beam directions.

where, β_0 and ϕ_0 are the elevation and azimuth angles with the main beam of the antenna points, β_{3dB} and ϕ_{3dB} are the vertical and horizontal 3dB beam widths of the main beam, respectively. F_0 is the average side lobe level of the antenna.

According to the calculation methods of scatter propagation mode and propagation energy proposed above, the scatter ionograms with the direction of the transmitting and the receiving beam are synthesized in this paper. The simulation examples are shown in Figure 10 and Figure 11.

From the simulation results, the smaller angle between the transmitting and receiving main beams could cause the larger area covered by side scatter, the larger blind zone, and the larger maximum observable frequency (MOF). The sum of the group path distances from the transmitting and receiving stations in this area is also greater.

IV. CONCLUSION

In this study, using the established ionospheric quasi-backscatter detection experimental platform, the three-dimensional sweeping frequency ionogram under the quasi-backscatter system is obtained for the first time. Through the analysis of the experimental results, the quasi-backscatter detection system can solve the inversion accuracy problem caused by the time difference between the backscatter detection and the oblique detection. Therefore, the inversion accuracy of ionospheric characteristic parameters could be significantly improved. In addition, in this paper, ray tracing technology is also used to simulate the propagation mode and energy of side-scatter, and the scattering characteristics under the quasi-backscatter detection system are initially obtained. A large number of subsequent experiments need to be further carried out for verifying the simulated results.

ACKNOWLEDGMENT

The authors are very grateful to China Research Institute of Radio Wave Propagation (CRIRP) for providing the ionosphere vertical detection data. Author contributions are as follows: conceptualization: Peng Lou and Lixin Guo, methodology: Jing Feng, software: Peng Lou, validation: Peng Lou, Jing Feng, and Na Wei, formal analysis: Na Wei, investigation: Peng Lou, data curation: Jing Feng, writing (original draft preparation): Peng Lou, writing (review and editing): Lixin Guo and Peng Lou, visualization: Jing Feng, supervision: Na Wei, and project administration: Lixin Guo. All authors have read and agreed to the published version of the manuscript.

REFERENCES

[1] R. Tiwari, H. J. Strangeways, S. Tiwari, and A. Ahmed, ''Investigation of ionospheric irregularities and scintillation using TEC at high latitude,'' *Adv. Space Res.*, vol. 52, no. 6, pp. 1111–1124, Sep. 2013.

[2] M. C. Kelly, *The Earth's Ionosphere: Plasma Physics and Electrodynamics*. San Diego, CA, USA: Academic, 2009.

[3] K. Davies, *Ionospheric Radio*. London, U.K.: Peter Peregrinus Ltd, 1990.
[4] B. W. Reinisch and H. Xueqin, "Automatic calculation of electron density profiles from digital ionograms: 3. Processing of bottomside ionograms," *Radio Sci.*, vol. 18, no. 3, pp. 477–492, May 1983.
[5] H. Xueqin and B. W. Reinisch, "Automatic calculation of electron density profiles from digital ionograms: 2. True height inversion of topside ionograms with the profile-fitting method," *Radio Sci.*, vol. 17, no. 4, pp. 837–844, Jul. 1982.
[6] B. W. Reinisch and H. Xueqin, "Automatic calculation of electron density profiles from digital ionograms: 1. Automatic O and X trace identification for topside ionograms," *Radio Sci.*, vol. 17, no. 2, pp. 421–434, Mar. 1982.
[7] M. H. Reilly and J. D. Kolesar, "A method for real height analysis of oblique ionograms," *Radio Sci.*, vol. 24, no. 4, pp. 575–583, Jul. 1989.
[8] G. F. Earl and B. D. Ward, "The frequency management system of the JINDALEE over-the-horizon backscatter HF radar," *Radio Sci.*, vol. 22, no. 2, pp. 275–296, 1987.
[9] B. W. Reinisch and D. M. Haines, "Ionospheric sounding in support of over-the-horizon radar," *Radio Sci.*, vol. 32, no. 5, pp. 1631–1694, 1997.
[10] T. A. Croft, "Sky-wave backscatter: A means for observing our environment at greatdistance," *Rev. Geophys. Space Phys.*, vol. 10, no. 1, pp. 73–155, 1972.
[11] C. J. Russell, P. L. Dyson, Z. Houminer, J. A. Bennett, and L. Li, "The effect of large-scale ionospheric gradients on backscatter ionograms," *Radio Sci.*, vol. 32, no. 5, pp. 1881–1897, Sep. 1997.
[12] T. J. Fuller-Rowell, G. H. Millward, A. D. Richmond, and M. V. Codrescu, "Storm-time changes in the upper atmosphere at low latitudes," *J. Atmos. Solar-Terr. Phys.*, vol. 64, nos. 12–14, pp. 1383–1391, Aug. 2002.
[13] J. Bremer, "Trends in the ionospheric E and F region over Europe," *Ann. Geophys.*, vol. 16, pp. 989–996, Aug. 1998.
[14] G. S. Bust and C. N. Mitchell, "History, current state, and future directions of ionospheric imaging," *Rev. Geophys.*, vol. 46, no. 1, pp. 1–23, 2008.
[15] A. D. Danilov, "Long-term trends in F2-layer parameters and their relation to other trends," *Adv. Space Res.*, vol. 35, no. 8, pp. 1405–1410, Jan. 2005.
[16] A. D. Danilov, "Long-term trends of F2 independent of geomagnetic activity," *Annales Geophys.*, vol. 21, no. 5, pp. 1167–1176, May 2003.
[17] A. D. Danilov and A. V. Mikhailov, "Spatial and seasonal variations of the for F2 long-term trends," *Ann. Geophys.*, vol. 17, pp. 1239–1243, Sep. 1999.
[18] A. J. Foppiano, L. Cid, and V. Jara, "Ionospheric long-term trends for south American mid-latitudes," *J. Atmos. Solar-Terr. Phys.*, vol. 61, no. 9, pp. 717–723, Jun. 1999.
[19] W. B. Gail, A. B. Prag, D. S. Coco, and C. Coker, "A statistical characterization of local mid-latitude total electron content," *J. Geophys. Res.*, vol. 98, no. A9, pp. 15717–15728, 1993.
[20] L. Peng, W. Shikai, F. Junmei, and J. Peinan, "The detection of traveling ionospheric disturbances by high-frequency backscatter sounding technique," *Acta Electronica Sinica*, vol. 40, no. 9, pp. 1900–1903, 2012.
[21] R. M. Jones, "A three-dimensional ray-tracing computer program," *Radio Sci.*, vol. 3, no. 1, pp. 93–94, Jan. 1968.
[22] C. J. Coleman, "A ray tracing formulation and its application to some problems in over-the-horizon radar," *Radio Sci.*, vol. 33, no. 4, pp. 1187–1197, Jul. 1998.
[23] J. Haselgrove, "Ray theory and a new method of ray tracing," *Phys. Ionosphere, Proc. Phys. Soc. London*, vol. 23, pp. 355–369, 1955.
[24] C. B. Haselgrove and J. Haselgrove, "Twisted ray paths in the ionosphere," *Proc. Phys. Soc. London*, vol. 75, no. 3, pp. 357–360, 1960.
[25] N. Y. Zaalov, E. M. Warrington, and A. J. Stocker, "A ray-tracing model to account for off–great circle HF propagation over northerly paths," *Radio Sci.*, vol. 40, no. 4, pp. 1–4, Aug. 2005.
[26] J. A. Bennett, "Variations of the ray path and phase path: A Hamiltonian formulation," *Radio Sci.*, vol. 8, pp. 737–741, Aug. 1973.
[27] M. Yao, G. Chen, Z. Zhao, Y. Wang, and B. Bai, "A novel low-power multifunctional ionospheric sounding system," *IEEE Trans. Instrum. Meas.*, vol. 6, no. 5, pp. 1252–1259, Dec. 2012.
[28] G.-J. Sun, D.-Y. Qi, and T.-C. Li, "Sea echo detection with the system of ionospheric backscatter sounding," *Acta Electronica Sinica*, vol. 33, no. 7, pp. 1334–1337, 2005.
[29] N. Wei, T.-C. Li, W. Liu, and J.-M. Fan, "An approach of suppressing non-long interference in HF backscatter system," *Acta Electronica Sinica*, vol. 38, no. 3, pp. 620–625, 2010.
[30] O. V. Fridman and S. V. Fridman, "A method of determining horizontal structure of the ionosphere from backscatter ionograms," *J. Atmos. Terr. Phys.*, vol. 56, no. 1, pp. 115–131, Jan. 1994.
[31] P. L. Dyson, "A simple method of backscatter ionogram analysis," *J. Atmos. Terr. Phys.*, vol. 53, nos. 1–2, pp. 75–88, Jan. 1991.
[32] L. J. Griffiths, "Time-domain adaptive beamforming of HF backscatter radar signals," *IEEE Trans. Antennas Propag.*, vol. AP-24, no. 5, pp. 707–720, Sep. 1976.
[33] Y. I. Abramovich, A. Y. Gorokhov, V. N. Mikhaylyukov, and I. P. Malyavin, "Exterior noise adaptive rejection for OTH radar implementations," in *Proc. IEEE Int. Conf. Acoust., Speech Signal Process. (ICASSP)*, Adelaide, SA, Australia, Apr. 1994, pp. 105–107.
[34] G. A. Fabrizio, Y. I. Abramovich, S. J. Anderson, D. A. Gray, and M. D. Turley, "Adaptive cancellation of nonstationary interference in HF antenna arrays," *IEE Proc. Radar, Sonar Navigat.*, vol. 145, no. 1, p. 19, 1998.
[35] G. A. Fabrizio, D. A. Gray, and M. D. Turley, "Experimental evaluation of adaptive beamforming methods and interference modes for high frequency over-the-horizon radar systems," *Multidimensional Syst. Signal Process.*, vol. 14, no. 1, pp. 241–263, 2003.
[36] Y. I. Abramovich, N. K. Spencer, S. J. Anderson, and A. Y. Gorokhov, "Stochasticconstraints method in nonstationary hot-clutter cancellation—Part 1: Fundamentals and supervised training applications," *IEEE Trans. Aerosp. Electron. Syst.*, vol. 34, no. 4, pp. 1271–1292, Oct. 1998.
[37] Y. I. Abramovich, N. K. Spencer, S. J. Anderson, and A. Y. Gorokhov, "Stochasticconstraints method in nonstationary hot-clutter cancellation—Part 2: Unsupervised training applications," *IEEE Trans. Aerosp. Electron. Syst.*, vol. 36, no. 4, pp. 132–150, Oct. 2000.
[38] J. R. Koster, "Some measurements on the sunset fading effect," *J. Geophys. Res.*, vol. 68, no. 9, pp. 2571–2578, May 1963.
[39] C. O. Hines and R. R. Rao, "Validity of three-station methods of determining ionospheric motions," *J. Atmos. Terr. Phys.*, vol. 30, no. 5, pp. 979–993, Jan. 1968.
[40] S. E. Appleton and W. R. Piggott, "Ionospheric absorption measurements during a sunspot cycle," *J. Atmos. Terr. Phys.*, vol. 5, nos. 1–6, pp. 141–172, Jan. 1954.
[41] B. H. Briggs, "On the analysis of moving patterns in geophysics—I. Correlation analysis," *J. Atmos. Terr. Phys.*, vol. 30, no. 10, pp. 1777–1788, Oct. 1968.
[42] M. R. Thorpe, "The phase integral correction for calculations of radio wave absorption in the ionosphere," *J. Atmos. Terr. Phys.*, vol. 33, no. 10, pp. 1597–1605, Oct. 1971.
[43] C. Little and H. Leinbach, "The riometer—A device for the continuous measurement of ionospheric absorption," *Proc. IRE*, vol. 47, no. 2, pp. 315–320, Feb. 1959.
[44] T. A. Croft and H. Hoogasian, "Exact ray calculations in a quasi-parabolic ionosphere with no magnetic field," *Radio Sci.*, vol. 3, no. 1, pp. 69–74, Jan. 1968.
[45] J. R. Hill, "Exact ray paths in a multisegment quasi-parabolic ionosphere," *Radio Sci.*, vol. 14, no. 5, pp. 855–861, Sep. 1979.
[46] K. Davies and C. M. Rush, "High-frequency ray paths in ionospheric layers with horizontal gradients," *Radio Sci.*, vol. 20, pp. 95–110, Jan. 1985.
[47] J. Caratori and C. Goutelard, "Derivation of horizontal ionospheric gradients from variable azimuth and elevation backscatter ionograms," *Radio Sci.*, vol. 32, no. 1, pp. 181–190, Jan. 1997.
[48] R. M. Jones, "A three-dimensional ray-tracing computer program (digest of ESSA technical report, ITSA No. 17)," *Radio Sci.*, vol. 3, no. 1, pp. 93–94, Jan. 1968.
[49] P. Lou, N. Wei, L. Guo, J. Feng, X. Li, and L. Yang, "Numerical study of traveling ionosphere disturbances with vertical incidence data," *Adv. Space Res.*, vol. 65, no. 4, pp. 1306–1320, Feb. 2020.
[50] K. Davies and D. M. Baker, "On frequency variations of ionospherically propagated HF radio signals," *Radio Sci.*, vol. 1, no. 5, pp. 545–556, 1966.
[51] K. G. Budden, *The Propagation of Radio Waves*. Cambridge, U.K.: Cambridge Univ. Press, 1985.
[52] J. G. Proakis, *Digital Communications*, 4th ed. New York, NY, USA: McGraw-Hill, 2001.
[53] M. H. Reilly, "Ionospheric true height profiles from oblique ionograms," *Radio Sci.*, vol. 20, no. 3, pp. 280–286, May 1985.
[54] O. V. Fridman, V. E. Nosov, and O. N. Boitman, "Reconstruction of horizontally-inhomogeneous ionospheric structure from oblique-incidence backscatter experiments," *J. Atmos. Terr. Phys.*, vol. 56, no. 3, pp. 369–376, Mar. 1994.
[55] J. Feng, B. Ni, P. Lou, N. Wei, L. Yang, W. Liu, Z. Zhao, and X. Li, "A new inversion algorithm for HF sky-wave backscatter ionograms," *Adv. Space Res.*, vol. 61, no. 10, pp. 2593–2608, May 2018, doi: 10.1016/j.asr.2018.03.002.

PENG LOU was born in Pingdingshan, China, in 1982. He received the B.S. degree in communication engineering from Northwestern Polytechnical University, Xi'an, Shanxi, China, in 2005, and the M.S. degree in electromagnetic fields and microwave technology from China Research Institute of Radio Wave Propagation (CRIRP), Qingdao, Shandong, China, in 2008. He is currently pursuing the Ph.D. degree in radio physics with Xidian University. In July 2008, he joined CRIRP, where he is currently a Senior Engineer. His current research interests include characteristics of HF propagation channel, HF radar, and ionospheric propagation.

LIXIN GUO (Senior Member, IEEE) received the M.S. degree in radio science from Xidian University, Xi'an, China, in 1993, and the Ph.D. degree in astrometry and celestial mechanics from the Chinese Academy of Sciences, Beijing, China, in 1999. He was a Visiting Scholar with the School of Electrical Engineering and Computer Science, Kyungpook National University, Daegu, South Korea, from 2001 to 2002. He has been a Visiting Professor with the Laboratoire d' Energetique des Systemes et Precedes, University of Rouen, Mont-Saint-Aignan, France, and the Faculty of Engineering and Physical Sciences, The University of Manchester, Manchester, U.K. He has been the Chief Professor of the Innovative Research Team, Shaanxi, China, since 2014. He is currently a Professor and the Head of the School of Physics and Optoelectronic Engineering, Xidian University. He has authored and coauthored four books and over 300 journal articles. He was in charge of more than 30 projects. His current research interests include electromagnetic wave propagation and scattering in complex and random media, computational electromagnetics, inverse scattering, and antenna analysis and design. He is a fellow of the Chinese Institute of Electronics and the Physics Institute of Shaanxi Province, China. He was a recipient of the National Science Fund for Distinguished Young Scholars, in 2012, and a Distinguished Professor of Changjiang Scholars Program, in 2014.

JING FENG received the M.S. degree in computational mathematics from the University of Electronic Science and Technology of China, in 2006. She is currently pursuing the Ph.D. degree in space physics with Wuhan University. In April 2006, she joined China Research Institute of Radio Wave Propagation (CRIRP), Qingdao, China, where she is currently a Senior Engineer. Her main research interests include ionospheric physics and radio wave propagation.

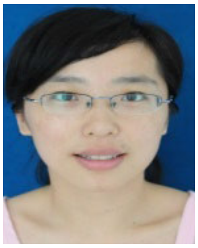

NA WEI was born in Shandong, China, in 1981. She received the Ph.D. degree in signal processing from Harbin Engineering University, China, in 2008. Her current research interests include radar signal processing and radio wave propagation.